Modern Management based on Big Data III
A.J. Tallón-Ballesteros (Ed.)

doi:10.3233/FAIA220116

Collaborative Control of Multi-Region Urban Traffic Boundary Based on the MFD

Yonghong XU[1]
Gansu Police Vocational College, China

Abstract. The increasing number of urban motor vehicle travel has brought more and more serious urban road traffic congestion in single region predicament. In order to study the traffic control problem of single-region urban network, a macroscopic model of traffic flow in urban region was constructed based on the macroscopic basic graph (MFD) theory to predict the traffic congestion pattern in urban region. In order to better explore the dynamic boundary control points, the queuing overflow of boundary sections was analyzed, and the regional boundary control strategy of real-time flow and queuing dynamics was given according to the real-time boundary morphology. In the case of improving and adjusting the signal timing of the input traffic flow at the boundary intersection, the regional traffic flow can be developed in a favorable direction, thus reducing the probability of overflow problems in the boundary section of the region, and contributing to the improvement of the overall operation efficiency of the region.

Keywords. MFD, congestion, multi-regional urban transport, control

1. Introduction

Macroscopic Fundamental Diagram (MFD) theory as a macroscopic modeling method for traffic flow on urban road networks is more suitable for developing traffic area control strategies and achieving optimal traffic flow efficiency on road networks[1]. Boundary control strategies based on MFD theory are one of the effective ways to deal with the regional traffic saturation or oversaturation dilemma. The control mechanism is to maintain the regional cumulative volume near the expected critical point by determining the boundary input flow to ensure the maximum volume of traffic within the region [2].

The boundary control strategy based on MFD is one of the effective means to solve the problem of regional traffic saturation or oversaturation. The main idea is to control the boundary input flow, maintain the regional accumulation near the desired key points, and achieve the maximum of regional traffic volume. In this paper, a MFD based dynamic boundary control strategy for single-region urban road network is proposed, in order to better solve the problems of signal control and road overflow at boundary intersections on the basis of improving the traffic operation capacity within the region.

In this paper, a MFD based dynamic boundary control strategy for single-region urban road network is proposed, in order to better solve the problems of signal

[1] Corresponding Author: Yonghong XU; Associate professor of Road Traffic Management, Department of Public Security, Gansu Police Vocational College; main research direction -- road traffic accident handling, traffic laws and regulations, etc.
E-mail: xuyonghong202205@163.com

control and road overflow at boundary intersections on the basis of improving the traffic operation capacity within the region. In the second part, the relevant model is constructed. In the third part, kalman filter method is used to realize the dynamic test of queuing length. In the fourth part, the simulation experiment and analysis of urban road traffic in a city of China are carried out, and the signal control improvement strategy of dynamic boundary intersection is given.

2. Construction of macro-model of regional traffic flow

Assume that there are two parts of a single-region urban road network, the congestion-protected area a and the area boundary b, where a is the central area of urban traffic, which undertakes the main function of urban traffic and often tends to be saturated or over-saturated form; the area boundary b represents all signal intersections around the congestion-protected area a. Then a macroscopic traffic flow graph for this city can be drawn as shown in Figure 1.

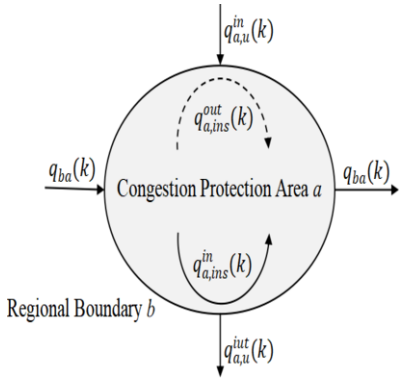

Figure 1 Macro traffic flow of single-region protection area a urban road network

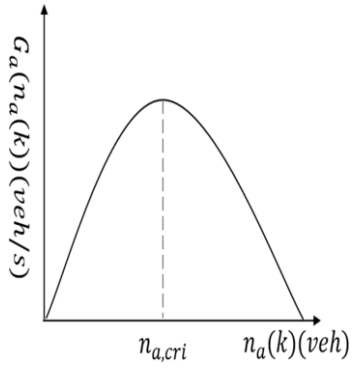

Figure 2 MFD diagram of congestion

First, set the observation time of the road network as an equal sequence of equal steps, i.e. $t = k \cdot T, k = 1,2,3,\ldots,k$, where T denotes the simulation time interval or boundary control interval, and expresses the dynamic process of regional traffic flow in terms of a simple conservation equation for the congestion protection region a, then we have

$$n_a(k+1) = n_a(k) + T(Q_{a,in}(k) - Q_{a,out}(k)) \qquad (2.1)$$

where $n_a(k)[veh]$ denotes the sum of traffic accumulation, or the total number of motor vehicles, in the region a at the kth time step; $Q_{a,in}(k)$ and $Q_{a,out}(k)[veh/s]$ denote the total input and output flows in the region a at the kth time step, respectively. Where $Q_{a,in}(k)$ is calculated as

$$Q_{a,in}(k) = q_{a,ins}^{in}(k) + q_{a,u}^{in}(k) - q_{ba}(k)) \qquad (2.2)$$

where $q_{a,ins}^{in}(k)[veh/s]$ denotes the total traffic demand within the region a at the kth time step; $q_{a,u}^{in}(k)[veh/s]$ denotes the uncontrolled input flow from region boundary b into region a at the kth time step; and $q_{ba}(k)[weh/s]$ denotes the controlled transfer flow from region boundary b to region a at the kth time step.

Second, $Q_{a,out}(k)$ represents the total of the uncontrolled output stream $q_{1,u}^{out}(k)$, the controlled transfer stream $q_{12}(k)$ and the trips ending within region a $q_{a,ins}^{out}(k)$. In addition, $Q_{a,out}(k)$ can also be replaced by the total trip completion rate of region a, $G_a(n_a(k))$, which is expressed by the equation

$$Q_{a,out}(k) = q_{a,ins}^{out}(k) + q_{a,u}^{out}(k) + q_{ab}(k) = G_a(n_a(k)) \quad (2.3)$$

From the composition of equation （1.3）, it can be seen that $G_a(n_a(k))$ is a non-negative, continuous, convex function with respect to the regional accumulation $n_a(k)(n_a(k) > 0)$, capable of representing the MFD relationship for the congestion-protected region a, as shown in Figure 2, which can be expressed as

$$G_a(n_a(k)) = xn_a^3(k) + yn_a^2(k) + zn_a(k) \quad (2.4)$$

where x, y and z denote the fitting parameters. The optimal critical accumulation $n_{a,cri}$ is derived from the fitted curve of the MFD and represents the regional accumulation consistent with the maximum trip completion rate.

Substituting equations (2.2) and (2.3) into equation (2.1) yields a discrete dynamic traffic flow equilibrium model for region a, as follows

$$n_a(k+1) = n_a(k) + T(q_{a,ins}^{in}(k) + q_{a,u}^{in}(k) + q_{ba}(k) - G_a(n_a(k))) \quad (2.5)$$

3. Real-time streaming and queuing dynamic area boundary control

The so-called boundary threshold, in essence, uses traffic lights to limit the number of motor vehicles entering the protected area of congestion to dynamically adjust the mobility of road network traffic, so as to realize the mechanism of eliminating regional traffic saturation or over-saturation in advance. For a single congestion area, Zhu et al. [3] proposed a discrete boundary feedback control strategy to effectively improve the traffic operation capacity of the road network. However, this strategy also has some shortcomings in practice: first, it fails to fully consider the dynamic characteristics of boundary controlled points; Second, the queuing overflow effect of boundary sections is ignored. Therefore, in the context of considering regional boundaries, this paper proposes a control strategy to optimize regional dynamic boundaries in order to improve traffic efficiency in congested areas.

3.1. Identification of Controlled Boundary Points

At boundary crossings in congestion protection areas, there are often multiple traffic control signals and each intersection presents different traffic operating state. If boundary control is implemented only at road sections with limited remaining storage space, the rate of occurrence of road section overflows problems will be significantly greater than in scenarios without boundary control, ultimately leading to the phenomenon of ineffective boundary control. For this reason, a dynamic boundary controlled point identification technique is required to counteract this.

Firstly, assuming that no traffic flow is generated or completed within the boundary section, i.e. no input port control is performed on all of the boundary sections, then traffic flow monitors are installed on all of the upper, middle and lower sections of the section, with the upper and lower sections functioning to measure real-time traffic flow and the middle section monitors functioning to obtain the hourly occupancy rate. In this case, the number of queuing motor vehicles can be predicted using the Kalman filter, which is given by the formula[4]

$$\hat{x}_{a,m}(k+1) = \hat{x}_{a,m}(k) + T(\mu_{a,m}(k) - q_{ba}^{m}(k)) + F(x_{a,m}(k) - \hat{x}_{a,m}(k)) \quad (3.1)$$

where m is the mth boundary section within the congestion protection area a; $\hat{x}_{a,m}(k)$ denotes the estimated queuing motor vehicle volume of the mth boundary section at the kth unit time; $\mu_{a,m}(k)$ denotes the real-time monitored arrival flow of the mth boundary section at the kth unit time; and $q_{ba}^{m}(k)$ denotes the real-time monitoring departure flow, i.e. the changing flow of the mth boundary section from area boundary b to protection area a; F denotes the fixed gain parameter of the Kalman filter. where the equation for real-time monitoring of queuing vehicles $x_{a,m}(k)$ is expressed as[5]

$$x_{a,m}(k) = N_{a,m}^{max} \cdot \frac{L_{ph}}{L_{ph}+\varepsilon} \cdot O_{a,m}(k) \quad (3.2)$$

Where $N_{a,m}^{max}$ denotes the maximum amount of motor vehicles that the mth boundary section can carry; $O_{a,m}(k)$ denotes the time occupancy of the middle monitor of the mth boundary section in the kth unit time; L_{ph} denotes the average value of motor vehicle length; ε denotes the effective range of the middle monitor. where $N_{a,m}^{max}$ denotes the criterion for judging whether the boundary crossing is controlled or not, and its calculation formula can be expressed as[6]

$$N_{a,m}^{max} = \frac{l_{a,m} \cdot \lambda_{a,m}}{L_{ph}} \quad (3.3)$$

where $l_{a,m}$ and $\lambda_{a,m}$ denote the length of the mth boundary section and the number of lanes on the road, respectively.

If $\hat{x}_{a,m}(k+1) < N_{a,m}^{max}$, it means that the mth boundary section meets the minimum requirements for being controlled and can be included in the set of boundary controlled points G_{k+1}; otherwise, the mth boundary section is classified as the set of boundary sections prone to overflow $\bar{G}_{k+1}$.

4. Simulation experiments and analysis of results

4.1. Experimental road network and simulation setup

In this paper, some areas of urban road traffic in a city were selected for simulation testing. Figure 3 shows a simplified diagram of the simulated road based on the VISSIM platform. The network consists of 55 road sections with 25 intersections, of which the points marked in a circle are the 15 boundary sections to be optimized. The data monitoring points for all sections of the area under test are located in the middle of the section, while the data monitoring points are also located upstream and downstream of the section. The core intersections in the area to be tested are marked with triangles and a four-phase signal timing scheme with a signal period of 180 s. The non-core intersections are timed with two phases and a period of 90 s. The speed of traffic in the test section is set between 45 km/h and 50 km/h according to the actual traffic conditions in the city chosen for the experiment.

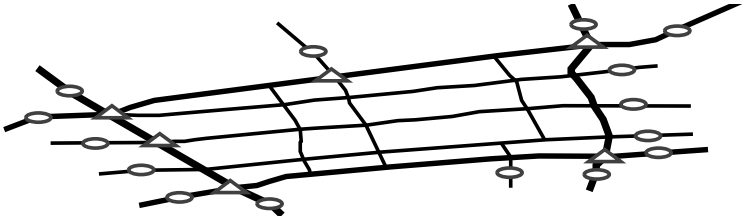

Figure 3. Simulation road network structure of the experimental area

4.2. Calculation of the optimal key accumulation quantity

To ensure the correctness of the MFD fitting results for the area to be tested, then a simulation of unbounded control is done. The traffic demand in the area to be tested is met with input flows from 15 boundary sections, as shown in Table 1. In this case, only a small amount of traffic enters the road network to begin with and increases in proportion to the traffic flow, eventually creating a traffic jam over a while.

Table 1 Input flow rate of the regional boundary section (Unit: veh/h)

Section	Simulation time(s)					
No.	0-900	900-1800	1800-3600	3600-5400	5400-7200	7200-14400
1	900	1800	3600	4800	5400	6000
2	300	600	1200	1600	1800	2000
3	600	1200	2400	3200	3600	4000
4	450	900	1800	2400	2700	3000
5	300	600	1200	1600	1800	2000
6	300	600	1200	1600	1800	2000
7	450	900	1800	2400	2700	3000
8	600	1200	2400	3200	3600	4000
9	300	600	1200	1600	1800	2000
10	750	1500	3000	4000	4500	5000
11	600	1200	2400	3200	3600	4000
12	150	300	600	800	900	1000
13	450	900	1800	2400	2700	3000
14	150	300	600	800	900	1000
15	450	900	1800	2400	2700	3000

Given the inherent randomness of the simulation results, six experiments were conducted under the same demand scenario, with a simulation time of 4h and a simulation step of 180s. Figure 4 shows the scatter plot of the simulation results for each random seed in the six experiments, represented as MFD-i (i=1,2,3,4,5,6). Each discrete point is the traffic accumulation and runs completion flow in the experimental area within 180s. Based on this data, the MATLAB tool was applied to fit the MFD of the experimental area, and the corresponding fitted curve was obtained as the solid grey line in Figure 5, whose curve model can be expressed as $G_a(n_a(k)) = 4.0852 \times 10^{-8} \times n_a^3(k) - 0.000394 \times n_a^b(k) + 0.9828 \times n_a$. The regional accumulation of vehicles reaches 1700 when it lies at the peak of the MFD curve, which is the maximum run completion rate. For this reason, 1700 vehicles are taken as the optimal critical accumulation in the dynamic boundary control strategy in this paper.

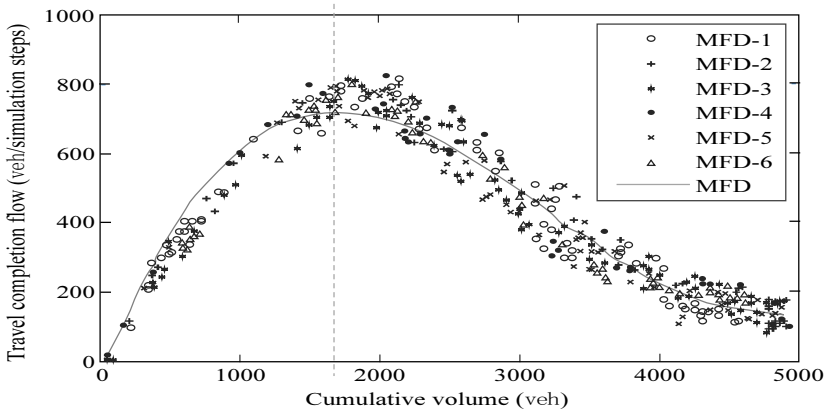

Figure 4 MFD fitting curve of the area to be measured

4.3. Simulation results and analysis of dynamic boundary control

Based on the above-mentioned traffic demand and optimal critical accumulation in the experimental area (Table 1), the duration of the simulation was determined to be 14,400 s with a step size of 180 s. Three different scenarios were simulated: first, a set of well-controlled timing schemes were set up in the experimental area without any traffic restrictions at the boundary intersections, and this scheme was regarded as the basic scheme, i.e., no boundary control, to facilitate comparison with other scenarios. The second is to use the same intersection signal control strategy as in the no-boundary control case, while the signal timing is modified with the boundary control strategy, i.e. the comparison scenario; the third is the proposed scheme with no-boundary control and dynamic boundary control, i.e. the approach of this paper.

The three experimental environments were set up with six replicate simulations each, and the effectiveness of each scenario was compared by regional run completion flows, average vehicle speeds and average delays. Table 2 shows the averages of the simulation results based on the three evaluation metrics, where the run completion flow represents the total number of motor vehicles leaving the experimental area in each simulation time unit; the averages of vehicle speed and delay are mainly shown for the full range including the boundary sections. The comparison with the no-boundary control case reveals that the proposed strategy in this paper improves the run completion flow by 45.90% and increases the average speed by 19.03%, which is higher than the 35.99% and 11.79% of the comparison method; the average delay under this paper's method is reduced by 35.47%, which is also greater than the 26.83% reduction of the comparison method. For this reason, the method in this paper contributes more to the operational effectiveness of the traffic flow compared to the comparison method and the borderless control.

Table 2 Comparative analysis of traffic operation performance

Performance Indicators	Boundaryless control	Comparison Method	Method of this paper	Comparison method improvement	Methodological improvements in this paper
Travel completion flow (veh)	416	569	602	35.99%	45.90%
Average speed (km/h)	26.98	31.07	31.25	11.79%	19.03%
Average delay (s/veh)	273	195	179	26.83%	35.47%

Figures 5 to 7 show the results of a single complete simulation under the three control strategies. It is not difficult to obtain the results from these plots: in the beginning, within a certain phase range (0 to 2300s), it is the kind of control strategy that has a similar effect, while as the number of vehicles approaches the optimal critical value, the boundary control strategy starts to be triggered, including the comparison method and the method of this paper.

Figure 5-1 indicates that the two boundary control scenarios would be triggered at 2300s, with different control results occurring with the input flows. As shown in Figure 5-2, the vehicle entry becomes less in the no-boundary control scenario due to traffic congestion. The boundary input flow under the control strategy of the comparison method also decreases significantly after several fluctuations and is similar to the no-boundary case for about half an hour, as shown in Figure 5-1. The dynamic boundary controlled strategy used in this paper exhibits more stable input flow control and is of better practical value.

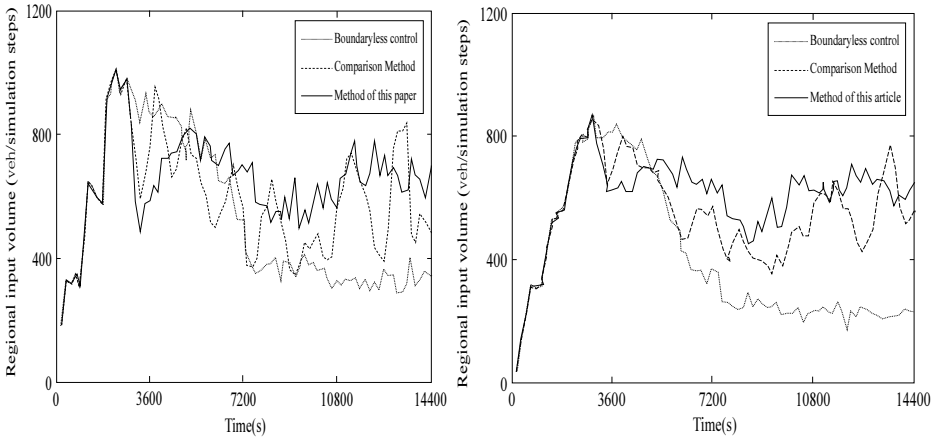

5-1 Regional input flow variation graph 5-2 Travel completion flow change graph

Figure 5 Boundary flow variation in the experimental area

Figure 7 shows the dynamics of the number of controlled boundary sections for the application of the method in this paper. Under the dynamic boundary control strategy, the proposed strategy is able to maintain the accumulation volume in the area to be measured around the optimal critical value. As can be seen from Figure 6, during the last 1h of the simulation, the actual accumulation volume under this strategy is not significantly different from the expected optimal critical value, which is significantly better than the comparison strategy. The dynamic change graph in Figure 5-2 also shows that during the last 1h, this method still marks a high output flow rate, which

is essentially the same as the change in accumulation in Figure 6. The method in this paper significantly outperforms the comparison method in terms of run completion flow for the simulation experiment.

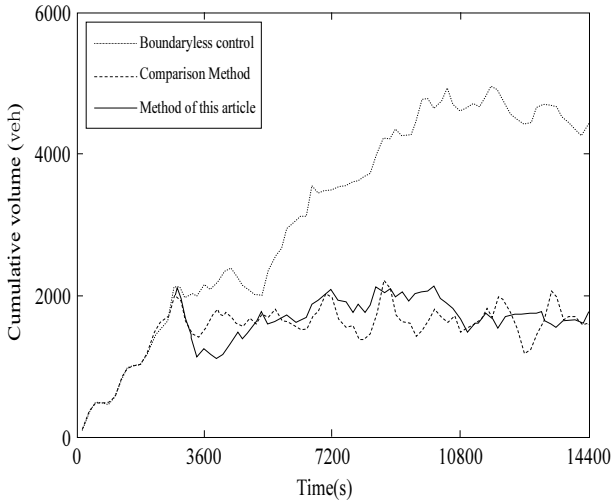

Figure 6 Variation of accumulation in the experimental area

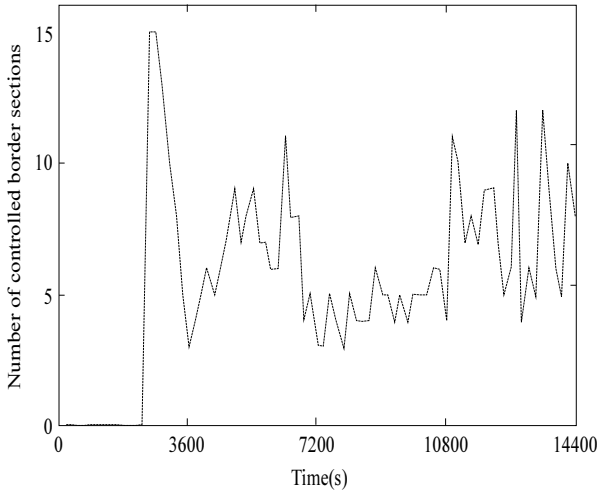

Figure 7 The variation of the controlled number of regional boundary sections of the method

5. Conclusion

Based on MFD theory, this paper proposes a regional dynamic boundary control strategy for the urban road congestion problem of single-region urban networks. Firstly, a traffic flow model to cope with a single congestion-protected region is constructed based on MFD theory; secondly, the Kalman filter method is applied to

realize real-time prediction of motor vehicle queue lengths on boundary sections and a dynamic boundary controlled point identification method is proposed; thirdly, based on the above two points, signal timing optimization of dynamic boundary intersections is given based on real-time flow and queue dynamics data at the regional boundary strategy.

References

[1] Sirmatel Isik Ilber et al. Modeling, estimation, and control in large-scale urban road networks with remaining travel distance dynamics[J]. Transportation Research Part C, 2021, 128

[2] Batista S.F.A. and Leclercq Ludovic and Menéndez Mónica. Dynamic Traffic Assignment for regional networks with traffic-dependent trip lengths and regional paths[J]. Transportation Research Part C, 2021, 127

[3] Zhu W X , Li S . Study on discrete boundary-feedback-control strategy for traffic flow based on Macroscopic Fundamental Diagram[J]. Physica a: Statal Mechanics and its applications, 2019, 523.

[4] G. Vigos, M. Papageorgiou, Y. Wang. Real-time estimation of vehicle-count within signalized links[J]. Transportation Research Part C: Emerging Technologies, 2008,16(1):18-35.

[5] Saad M Khaleel,Gandhi G Sofia,Ali J Kadhim. Development of Vehicle Queue Model for Selected Signalized Intersections at CBD in Sulaymaniyah City[J]. IOP Conference Series: Materials Science and Engineering,2019,518(2):1-8.

[6] Zhang Weihua, Chen Sen, Ding Heng. Feedback valve control considering traffic congestion at boundary intersection [J]. Control theory &applications,2019,36(02):241-248.